ELSEVIER

Contents lists available at ScienceDirect

Anthropocene

journal homepage: www.elsevier.com/locate/ancene





Recognizing flood exposure inequities across flood frequencies

Haley Selsor^{a,*}, Brian P. Bledsoe^a, Roderick Lammers^b

- ^a Institute for Resilient Infrastructure Systems, University of Georgia, 200 D.W. Brooks Drive, Athens, GA 30605, USA
- b School of Engineering and Technology and Institute for Great Lakes Research, Central Michigan University, ET 147, Mt. Pleasant, MI 48859, USA

ARTICLE INFO

Keywords: Flood risk equity Urban flood hazard Social vulnerability Environmental justice

ABSTRACT

Urban flooding is a growing threat due to land use and climate change. Vulnerable populations tend to have greater exposure to flooding as a result of historical societal and institutional processes. Most flood vulnerability studies focus on a single large flood, neglecting the impact of small, frequent floods. Therefore, there is a need to investigate inequitable flood exposure across a range of event magnitudes and frequencies. To explore this question, we develop a novel score of inequitable flood risk by defining risk as a function of frequency, exposure, and vulnerability. This analysis combines high-resolution, parcel-scale compounded fluvial and pluvial flood data with census data at the census block group scale. We focus on six census tracts within Athens-Clarke County, Georgia that are highly developed with diverse populations. We define vulnerable populations as non-Hispanic Black, Hispanic, and households under the poverty level and use dasymetric mapping techniques to calculate the over-representation of these populations in flood zones. Inequitable risks at each census tract (approximately neighborhood scale) were estimated for multiple (e.g., 5-, 10-, 20-, 50-, and 100-year) flood return periods. Results show that the relatively greatest flood risk inequities occur for the 10-year flood and not at the largest event. We also found that the size of inequity is dynamic, depending on the flood magnitude. Therefore, addressing a range of events including smaller, more frequent floods can increase equity and reveal opportunities that may be missed if only one event is considered.

1. Introduction

Flooding is one of the most costly and frequent natural disasters facing the United States, with 41 million people estimated to currently reside in flood prone areas (Wing et al., 2018). Climate and land use change are expected to increase flooding, especially in urban areas (Hollis, 1975; Huang et al., 2007; Trenberth, 2011; Kunkel et al., 2013; Zhou et al., 2019). The growing threat of flooding in urban communities is concerning considering that urban populations are growing simultaneously. The United Nations predicts that 90% of the North American population will live in urban areas by 2050 (United Nations Population Division, 2008). Without adequate adaptations, escalating flood exposure will threaten both a city's built environment and residents.

The harmful and long-lasting impacts of flooding are not experienced equally across communities (Coninx and Bachus, 2021). Socially vulnerable populations are commonly characterized by low-incomes, racial and ethnic minorities, limited education, disabilities, ages under 16 and over 75, and/or single-parent households, and they bear the burdens of flooding, having been delegated to flood prone areas (Bigi

et al., 2021; Debbage, 2019; Qiang, 2019). While they face greater exposure, socially vulnerable populations possess limited access to resources and support structures to respond to floods, diminishing resilience and prolonging recovery (Rufat et al., 2015). The existing flood exposure disparities will only be exacerbated by climate change (Mason et al., 2017; Rickless et al., 2020; Shepherd and KC, 2015; Wing et al., 2022). This is especially true in the Southeast United States where historical racism and segregation have led to greater flood exposure for Black and African American communities (Cutter et al., 2003; Linscott et al., 2021; Tate et al., 2021; Ueland and Warf, 2006).

To identify the inequities in flood exposure, many studies overlay flood exposure maps with a social vulnerability index to locate spatial coincidence of highly vulnerable populations and high flood risk (Chakraborty et al., 2014; Coninx and Bachus, 2021; Koks et al., 2015; Nelson et al., 2015; Tascón-González et al., 2020). These studies typically investigate only a single flood magnitude, often the 100-year flood or a historical flood, producing spatial depictions of flood risk that are only applicable to one specific event. Nuisance flooding is the small, frequent flood events that can cause more cumulative damage over time

E-mail address: hks47033@uga.edu (H. Selsor).

^{*} Corresponding author.

H. Selsor et al. Anthropocene 42 (2023) 100371

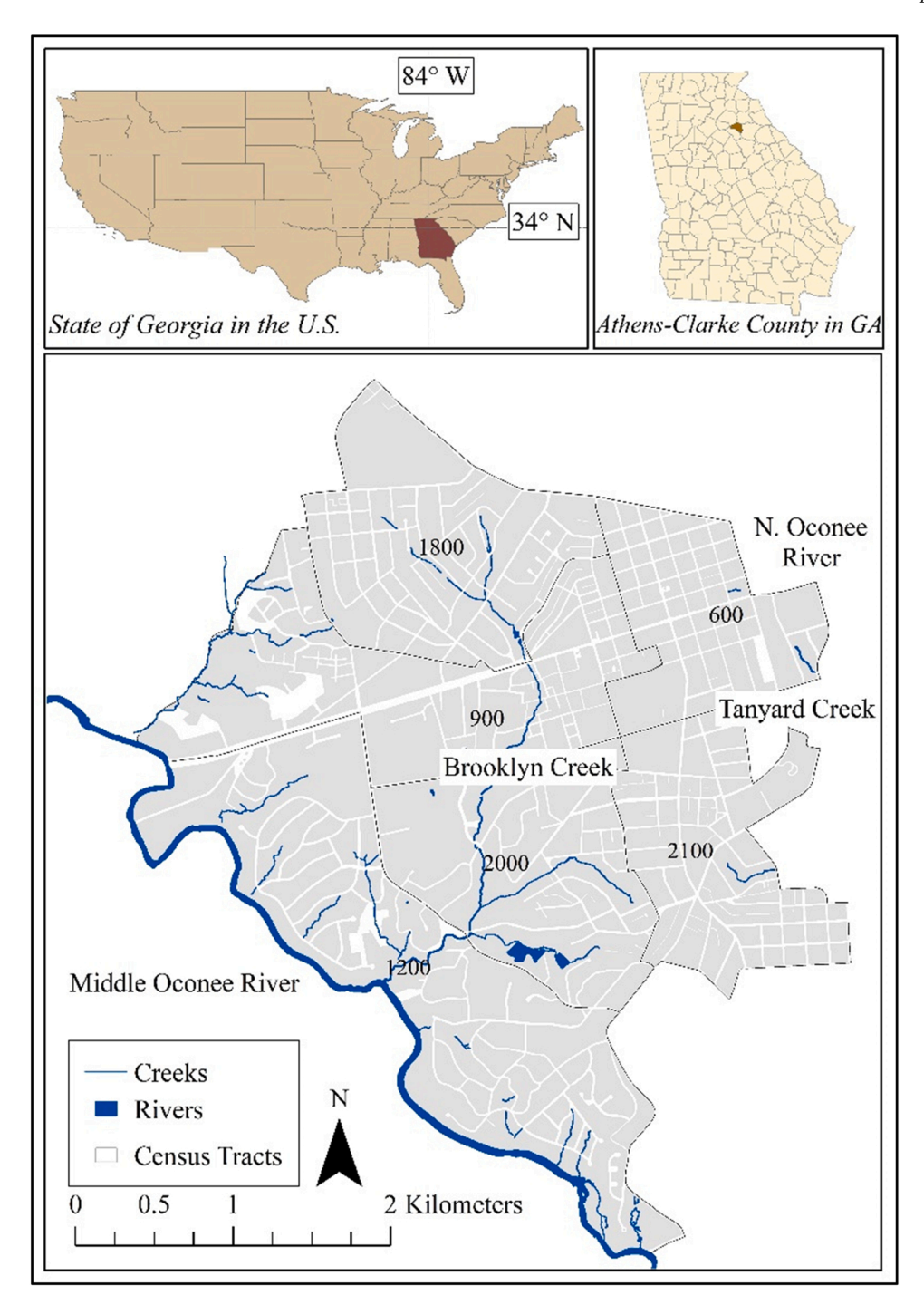


Fig. 1. The six census tracts overlapping Brooklyn Creek Watershed and the sources of riverine flooding.

than a large, single event, and is a challenge for urban areas (Moftakhari et al., 2017, 2018). Nuisance flooding represents a category of flooding for which inequity has not been investigated. For this reason, there is a need to look at flood inequity across multiple flood magnitudes that captures the impacts of the small, but frequent floods.

In a review of studies that analyzed flood risk using multiple return periods, we found they generally follow the same methodology where flood risk is the product of exposure and social vulnerability. A return period is analogous to a recurrence interval, and this term is used interchangeably with flood magnitude as a larger return period corresponds to a large, infrequent flood. Multiple papers integrate exposure from multiple return periods into a single flood exposure index and while this is useful for planning purposes, the reader cannot distinguish

how risk changes across flood magnitudes (Chakraborty et al., 2005; Künzler et al., 2012; Vicente et al., 2006; Wing et al., 2022). Other studies produced risk maps separately for different return periods using separate flood exposure inputs but do not look at a wide range of events (Abdrabo et al., 2020; Liu et al., 2021). There are a few papers that employed different methods for estimating risk. Some studies incorporated exposure as indicators (e.g., percent of flooded area, flood depth, tidal range, etc.) with the social vulnerability indicators into a single index instead of using a flood map or flood index to calculate risk (Hadipour et al., 2020; Ye et al., 2022). Additionally, a few papers used exposure maps with depth-damage curves to estimate economic damages in the form of income loss, cost of repairs, etc. for different return periods (Schuster-Wallace et al., 2018; Tyagi, 2020; Yang et al., 2020).

One paper did conduct a flood equity analysis in the Liege province of Belgium, and they found that the lower to middle socio-economic status populations were more exposed to flooding (Poussard et al., 2021). The authors end their study by stating the need for further research on the relationship between flood frequencies and socioeconomic characteristics (Poussard et al., 2021).

In the studies where flood risk was analyzed separately for multiple return periods, risk increases with return period (Abdrabo et al., 2020; Liu et al., 2021; Ye et al., 2022). These findings are reasonable because in all these instances, the exposure input (flood inundation) changed while the social vulnerability indicators remained the same. As flood exposure expands, risk increases. The social vulnerability indices values remained the same even though the population impacted by a flood may change with flood magnitude. For this reason, we employed methods from Debbage (2019) to calculate social vulnerability based on the disproportionate presence of socially vulnerable populations in the flood zone for each event separately. This allows us to incorporate social vulnerability in our analysis by accounting for how the demographics of the exposed population change according to inundation patterns from different size floods.

In this paper, we investigate the trends in flood inequity across multiple flood frequencies. We use the framework that risk is a function of hazard, exposure, and vulnerability and define hazard as the likelihood of an certain flood magnitude occurring and exposure as the Brooklyn Creek watershed is demographically diverse and is made up of a mix of income levels, races, and ethnicities. We selected this area based on a preliminary study of Athens-Clarke County that compared flood exposure and demographics across the county (Selsor et al., 2021). We found that land cover of this area is 70% developed, resulting in larger runoff amounts that can lead to great flood exposure than less developed areas of the county. Flooding in these selected tracts is from rainfall and several streams: Brooklyn Creek, Middle Oconee River, Tanyard Creek, and the North Oconee River.

2.2. Flood inequity (FI) score

We developed a Flood Inequity score by applying our own definitions to modify the standard risk equation to measure equity with Eq. 1. The proposed score is scaled between zero and one and produces relative inequity among the six census tracts. A FI score of zero indicates that the distribution of flood exposure is apparently equitable, and any score above zero indicates inequitable distribution with the socially vulnerable bearing a disproportionate amount of the exposure. Because we are measuring the equity associated with flooding, and not flood risk itself, a score of zero means the area has equitable flood exposure, not that there is no flooding. We calculated the FI score for the 5-, 10-, 20-, 50-, and 100-yr return periods for each census tract in the study area.

Flood Inequity = Likelihood of flood x damages from flood x overrepresenation of socially vulnearble population in flood zone

(1)

damages caused by this flood magnitude (Joyce et al., 2018; Kaźmierczak and Cavan, 2011; Koks et al., 2015; Kron, 2005; Preisser et al., 2022). We apply a unique definition of vulnerability as the overrepresentation of socially vulnerable population in the flood zone compared to non-socially vulnerable populations. The conceptualization of vulnerability is not based on static indicators, but changes with return period. Vulnerability is made up of the components of exposure, adaptive capacity, and sensitivity and as a concept can be applied to a variety of spheres to describe the ability to cope with different environmental hazards, including social, technological, and ecological vulnerability (Chang et al., 2021). (Bigi et al., 2021; KC et al., 2015). We focus on social vulnerability, and while we do include exposure in our conceptualization, we opted to not differentiate between sensitivity and adaptive capacity because the focus of our study is on evaluating equity. Defining social vulnerability further by distinguishing between adaptive capacity and sensitivity would have introduced more complexity than was necessary to answer our research questions. Using high resolution, parcel level flood data produced from modeled compound fluvial and pluvial flooding, we build on the work of Debbage (2019) to develop a novel metric to evaluate flood inequity. The flood inequity analysis will answer the following questions: (1) How does flood exposure inequity vary with flood magnitude, and (2) Which flood magnitude produces the largest inequities? We hypothesize that flood exposure inequity will be the greatest for the smaller flood magnitudes and will steadily decline until the 100-year event.

2. Methods

2.1. Study site

The study site for this paper is six census tracts overlapping the Brooklyn Creek watershed in Athens-Clarke County, Georgia (Fig. 1). This $13.2~{\rm km}^2$ area is highly developed with a mix of residential and commercial development that includes a hospital, a public library, and three public schools that provide critical services to the community.

2.3. Likelihood x damages

When calculating the likelihood of a flood's occurrence, we used the probability of a specific flood magnitude occurring at least once within 30 years using Eq. 2 (Bedient et al., 2008). We opted to use this probability because it is the likelihood a flood will occur over a time period which is more representative of a resident living in a neighborhood for several years than the likelihood it will occur at least once in any given year. In Eq. 2, Tr is the return period in years and n is the planning horizon in years (Bedient et al., 2008).

Likelihood of flood =
$$1 - \left(1 - \frac{1}{T_r}\right)^n$$
 (2)

To approximate the damages associated with an event, we used the median depth of flooding at buildings within the census tract, which can result in long-term health effects, emotional stress, and financial burden (Convery and Bailey, 2008; Wilson et al., 2021). We used flood data from First Street Foundation that models pluvial and fluvial flooding across the continental United States to estimate flood inundation and depth at the parcel scale (First Street Foundation, 2020). The First Street Foundation data were generated with the LISFLOOD-FP model that employs an inertial formulation of the shallow water equations to route floods and generate an inundation area based on assumptions of rectangular channel geometry, uniform channel bed-slope, and uniform friction factor (Bates and De Roo, 2000; Wing et al., 2017). The modeling provides inundation depths for each parcel at the lowest elevation of the building footprint for multiple return periods. We chose the First Street dataset because it covers multiple return periods using consistent data and modeling approach unlike the Federal Emergency Management Agency (FEMA) Flood Insurance Rate Maps (FIRM) which provide flood extents for only the 100-yr and 500-yr events with inconsistent updates. To more directly consider damages to the community, we only used parcels with flood inundation that reached a building. We included flood depths at all buildings, not just residential

Table 1The demographic populations compared in each exposure ratio, and the meaning of the results.

| Exposure Ratio | Population #1 | Population #2 | Meaning of Results |
|-------------------|--|--|---|
| Race | non- Hispanic Black Population | non-Hispanic white Population | If exposure ratio > 1, non- Hispanic Black population overrepresented |
| Ethnicity | Hispanic Population | Non-Hispanic Population | If exposure ratio > 1, Hispanic population overrepresented |
| Income | Households under the poverty level | Households above the poverty level | If exposure ratio > 1, low- income population overrepresented |

buildings, because damages to other types of development (e.g., schools, grocery stores, businesses, etc.) can impact access to education, food, and other necessities that would not be captured by looking at residences alone.

In ArcMap (Version 10.3.1), we spatially joined the flood depths point file with a parcel shapefile of the area (Esri Inc, 2015). We filtered out parcels with buildings and imported that flood data to calculate the median depth of flooding within each tract for each return period. We had to calculate the median flood depth to match the scale of the vulnerability calculations which are at the census tract scale. We classified the median flood depths across all scenarios into bins using natural breaks to prevent inflation of the least and worst-case scenarios (Moreira et al., 2021; Preisser et al., 2022). We used the BAMMtools package in R to calculate the thresholds for Jenks natural breaks (R Core Team, 2022; Rabosky et al., 2014).

2.4. Vulnerability

Studies of flood risk in the Southern United States found that non-Hispanic Black, Hispanic, other racial and ethnic minorities, and populations under the federal poverty level experienced significantly greater flood risk (Chakraborty et al., 2019; Collins et al., 2019; Debbage, 2019; Linscott et al., 2021). Ueland and Warf (2006) found that Black and African American communities are concentrated in low-lying areas and have greater flood risk. In a study of the state of Georgia, KC et al. (2015) found that Athens-Clarke County is moderately vulnerable to climate change and corresponding rainfall changes and explains that as a "Black Belt" county, Athens-Clarke County has a high African American population with an increasing Hispanic population. Because of the prevalence of Black, Hispanic, and low-income communities with disproportionate flood risk throughout the South, we chose to use these characteristics as the three dimensions of social vulnerability. We downloaded the non-Hispanic Black, non-Hispanic White, Hispanic, non-Hispanic, households under the poverty level, and total number of households data for each census block group from the American Community Survey 2018 5-year estimates (U.S. Census Bureau, 2019a, 2019b, 2019c). We used a 5-year estimate instead of a single year because this reduces the uncertainty in survey data at small scales (Spielman et al., 2014).

We included the inundation extent for each scenario with dasymetric mapping to calculate vulnerability, producing different vulnerability values for each flood magnitude (Debbage, 2019; Maantay and Maroko, 2009). With dasymetric mapping, the proportion of flooded, developed area becomes a factor that corresponds to the proportion of the flood exposed population within a census block group (Harner et al., 2002). To account for heterogeneity in the distribution of people, we applied the urban-filtering technique to filter land cover types and only use developed area when calculating the factor. This prevents the overestimation of exposed populations in the flood zone (Debbage, 2019). We assigned a land cover type to each parcel based on the majority of the land cover cells within the parcel from the National Land Cover

Table 2 Results of the exposure ratio for each tract and different flood return periods, with statistically significant results starred (alpha = 0.1).

| Tract | Flood Return Period | Race | Ethnicity | Income |
|-------|---------------------|--------|-----------|--------|
| 600 | 5 | n/a | n/a | n/a |
| | 10 | 2.19 * | 0.46 | 0.96 |
| | 20 | 1.90 * | 0.56 | 0.96 |
| | 50 | 2.34 * | 0.42 * | 0.95 |
| | 100 | 2.34 * | 0.42 * | 0.95 |
| 900 | 5 | 0.81 | 2.00 | 0.77 |
| | 10 | 2.01 * | 0.86 | 1.16 |
| | 20 | 1.54 * | 0.72 | 1.18 |
| | 50 | 1.56 * | 0.72 | 1.18 |
| | 100 | 1.56 * | 0.72 | 1.18 |
| 1200 | 5 | 1.11 | 1.15 | 1.06 |
| | 10 | 1.14 | 1.19 | 1.07 |
| | 20 | 1.18 | 1.24 | 1.09 |
| | 50 | 1.19 | 1.24 | 1.09 |
| | 100 | 1.19 | 1.24 | 1.09 |
| 1800 | 5 | 0.50 | 0.57 | 0.71 |
| | 10 | 1.21 | 0.23 * | 0.76 |
| | 20 | 1.20 | 0.23 * | 0.76 |
| | 50 | 1.18 | 0.24 | 0.76 |
| | 100 | 1.18 | 0.24 | 0.76 |
| 2000 | 5 | 0.04 | 0.27 | 0.15 |
| | 10 | 1.59 | 1.39 | 1.45 * |
| | 20 | 1.57 | 1.38 | 1.43 * |
| | 50 | 1.60 * | 1.40 | 1.45 * |
| | 100 | 1.60 | 1.40 | 1.45 |
| 2100 | 5 | 0.62 | 0.98 | 0.79 |
| | 10 | 0.75 | 0.99 | 0.84 |
| | 20 | 1.00 | 1.00 | 1.00 |
| | 50 | 1.00 | 1.00 | 1.00 |
| | 100 | 1.00 | 1.00 | 1.00 |

Database 2016 30 m resolution land use raster (Homer et al., 2020). Only parcels with a majority land cover type of developed open spaces, developed low intensity, developed medium intensity, or developed high intensity (Types 21–24) were included in calculating the factors of proportion of developed, flooded area, for each census block group.

This factor was multiplied by each population of interest (i.e., non-Hispanic Black, non-Hispanic White, Hispanic, non-Hispanic, households under the poverty level, and total number of households) in each block group to determine the exposed population for each block group. The census tract exposed population is the sum of its block group exposed populations. An Exposure Ratio (ER) compares the presence of two different demographics in the flood zone within census tract (Eq. 3) to determine if one is overrepresented. Each exposed population of a certain demographic is normalized by the total population of that demographic, so the results are not influenced by the size of one population being larger than the other. We performed the comparisons listed in Table 1. We calculated all three ERs (i.e., Race, Ethnicity, and Income) and corresponding p-values for each census tract and return period using the fmsb package in R (Nakazawa, 2019; R Core Team, 2022). We tested a null hypothesis of independence between flood exposure and socio-demographic characteristics and used a significance threshold of $p \leq 0.1$ to reduce the likelihood of Type-II errors (false negatives), where there is over-representation of vulnerable populations in the flood zone, but it is not considered statistically significant.

$$Exposure Ratio = \frac{\substack{exposed \ population\#1\\ total \ population\#2}}{\substack{total \ population\#2\\ total \ population\#2}}$$
(3)

We aggregated the exposure ratios into a single value to describe vulnerability. We attempted aggregation with four different methods and compared them with a sensitivity analysis in more detail in the Appendix. We selected the method where ERs less than one were reassigned a value of one, and ratios greater than one were left as-is, and then the three ratios were summed. Reassigning the values less than one

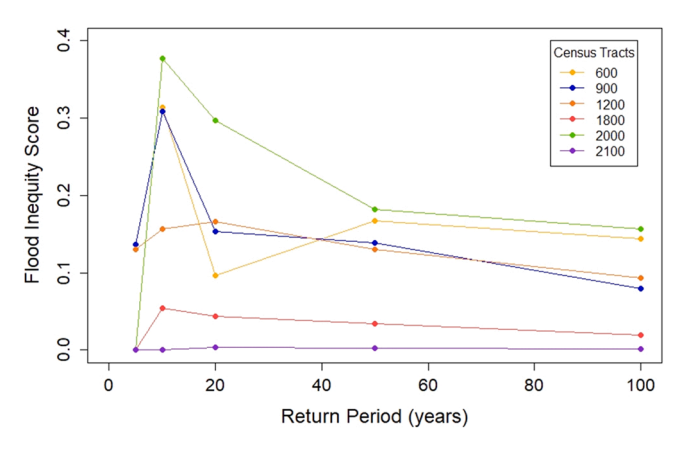


Fig. 2. A plot of FI scores versus return periods for each tract. Each point marks a flood event for which the flood inequity score was calculated as a function of the likelihood and extent of damages occurring for an event and the over-representation of vulnerable populations in the flood zone for that event.

Table 3Flood inequity scores for census tracts across the return periods

| Census Tract | Flood Return Period | Likelihood | Damages | Vulnerability | Flood Inequity Score |
|-----------------|---------------------------|------------|---------|---------------|----------------------------|
| 600 | 5 | 0.999 | 0 | n/a | n/a |
| | 10 | 0.958 | 0.4 | 0.819 | 0.314 |
| | 20 | 0.785 | 0.2 | 0.618 | 0.097 |
| | 50 | 0.455 | 0.4 | 0.919 | 0.167 |
| | 100 | 0.260 | 0.6 | 0.919 | 0.144 |
| 900 | 5 | 0.999 | 0.2 | 0.686 | 0.137 |
| | 10 | 0.958 | 0.4 | 0.805 | 0.308 |
| | 20 | 0.785 | 0.4 | 0.490 | 0.154 |
| | 50 | 0.455 | 0.6 | 0.509 | 0.139 |
| | 100 | 0.260 | 0.6 | 0.509 | 0.079 |
| 1200 | 5 | 0.999 | 0.6 | 0.218 | 0.130 |
| | 10 | 0.958 | 0.6 | 0.273 | 0.157 |
| | 20 | 0.785 | 0.6 | 0.353 | 0.166 |
| | 50 | 0.455 | 0.8 | 0.357 | 0.130 |
| | 100 | 0.260 | 1 | 0.357 | 0.093 |
| 1800 | 5 | 0.999 | 0.2 | 0.000 | 0.000 |
| | 10 | 0.958 | 0.4 | 0.141 | 0.054 |
| | 20 | 0.785 | 0.4 | 0.140 | 0.044 |
| | 50 | 0.455 | 0.6 | 0.125 | 0.034 |
| | 100 | 0.260 | 0.6 | 0.125 | 0.020 |
| 2000 | 5 | 0.999 | 0.2 | 0.000 | 0.000 |
| | 10 | 0.958 | 0.4 | 0.984 | 0.377 |
| | 20 | 0.785 | 0.4 | 0.947 | 0.297 |
| | 50 | 0.455 | 0.4 | 1.000 | 0.182 |
| | 100 | 0.260 | 0.6 | 1.000 | 0.156 |
| 2100 | 5 | 0.999 | 0.2 | 0.000 | 0.000 |
| | 10 | 0.958 | 0.8 | 0.000 | 0.000 |
| | 20 | 0.785 | 1 | 0.005 | 0.004 |
| | 50 | 0.455 | 1 | 0.005 | 0.002 |
| | 100 | 0.260 | 1 | 0.005 | 0.001 |

prevented the masking of over-represented socially vulnerable populations if one ER was high and the other two were less than one. Reassigning the values also allowed for a clear threshold to distinguish from an equitable distribution to an inequitable distribution of flood. We normalized the aggregate values using min-max normalization (Moreira et al., 2021). The individual ERs are weighted equally because weighting is the greatest source of uncertainty in aggregating social vulnerability indicactors, and the inclusion of a weighting scheme would introduce subjectivity in considering one vulnerable population (e.g., Hispanic) more vulnerable than another (e.g., low-income) (Rufat et al., 2015, 2019; Tate, 2012, 2013).

3. Results

3.1. Statistical significance of exposure ratios

While it was difficult to determine statistical significance of the exposure ratios due to small population sizes at the census tract scale, we were able to produce fine resolution results. Four of the six census tracts have a statistically significant exposure ratio in at least one scenario (Table 2). The largest, significant ER is 2.3 for the non-Hispanic Black population in Tract 600 for the 50-year event. The ratio of 2.3 means the non-Hispanic Black population is 2.3 times more likely to reside in the flood zone than the non-Hispanic white population. The greatest statistically significant ratios were over 2.0, and all four of these were race ERs.

Tract 900 and Tract 2000 have significant ratios that are greater than one, which means there are vulnerable populations over-represented in the flood zone within these tracts. Tract 1800 has a significant ratio that is less than one, which means that the non-vulnerable population is more likely to reside in the flood zone. Tract 600 has both a statistically significant race ER greater than one and a significant ethnicity ER less than one. Overall, the most extreme exposure ratios, with the greatest over-representation, are statistically significant while the smaller exposure ratios that are close to one are not statistically significant.

3.2. Flood inequity score

We identified inequities in all but one census tract with some tracts showing relatively larger flood inequities within our study, indicating that some census tracts have a more equitable distribution of flooding than others. The largest inequity occurs during the 10-year event for four out of six census tracts and for the 20-year event for the other two tracts (Fig. 2, Table 3). We also observed that the ranges and patterns of flood inequity scores across the flood magnitudes vary for the tracts. For Tracts 600, 900, and 2000, the FI scores are the largest for the 10-year event, while Tracts 1200, 1800, and 2100 have much smaller variation in their FI scores across the return periods. The FI scores peak at the 10-year event for Tracts 600, 900, and 2000 and then become asymptotic for larger, less frequent events. After the peak, the behavior of the FI score varies until the 50-year event for all tracts. Generally, as the flood magnitudes increase beyond the 20-year event, the changes in the FI scores are less drastic, and the FI score approaches an asymptotic value for each tract. The spatial distribution of FI scores for the 10-year and 100-year event are compared in Fig. 3. Additionally, the tracts with significant ERs (i.e. Tract 600, 900, 2000), with over-representation of vulnerable populations in the flood zone, demonstrate the greatest variation in the FI score across the return periods.

For comparison, we summed the Flood Inequity scores and damages across the return periods to compare exposure and equity of the census tracts. Tract 2100 has the highest exposure total of the tracts, but its FI total is almost zero because the vulnerability values are zero, which means all populations have equal flood exposure (Table 4). Tract 1200 has the second highest exposure total, but has lower vulnerability values, so the FI total is in the middle range. Tracts 900 and 1800 have identical exposure values for each return period, but very different FI scores because 1800 has low vulnerability values and Tract 900 has high vulnerability values. Tract 2000 has the second to last lowest exposure total, but its high vulnerability values result in it having the highest FI total across all tracts. Tract 600 has the lowest exposure total and the lack of flooding at buildings for the 5-year event could be a contributing factor. While Tract 600's exposure total was the lowest, it has some of the highest vulnerability values, so the FI scores are high.

4. Discussion

It is typical for flood vulnerability assessments to use the 100-year flood zone or worst-case scenario of flooding under the assumption

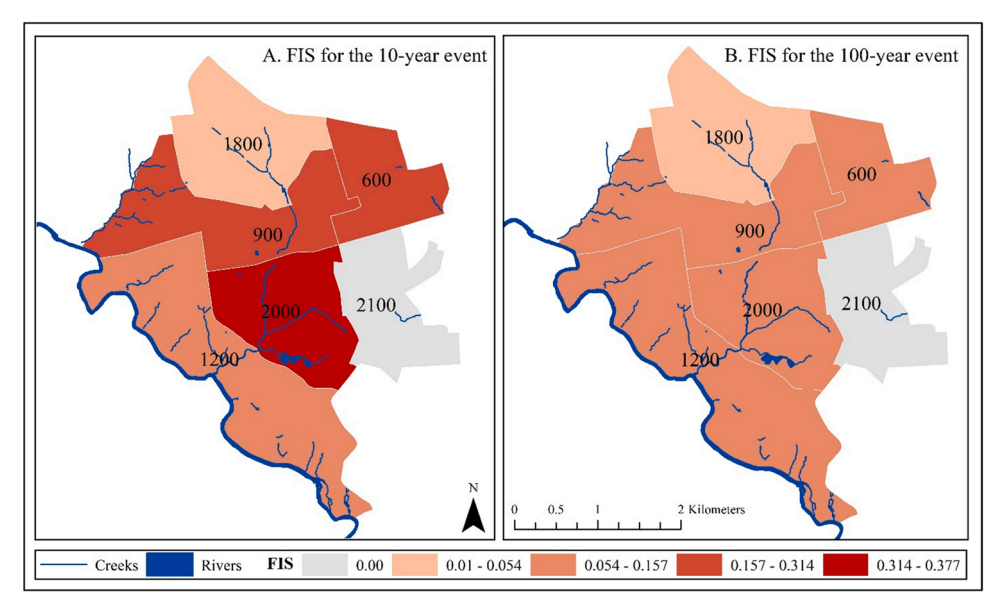


Fig. 3. A map of flood inequity scores, comparing the results for the 10-year event and the 100-year event. The darkest red area has the greatest inequity and the gray areas have the most equitable flood distribution.

Table 4
Ranks of tracts from highest to lowest exposure total and highest to lowest FI total.

| Exposure Total | Tract | FI Total | Tract |
|----------------|-------|----------|-------|
| 4 | 2100 | 1.01 | 2000 |
| 3.6 | 1200 | 0.82 | 900 |
| 2.2 | 900 | 0.82 | 600 |
| 2.2 | 1800 | 0.68 | 1200 |
| 2 | 2000 | 0.15 | 1800 |
| 1.8 | 600 | 0.01 | 2100 |

that the worst-case scenario of flooding reveals the most extreme inequities. However, we found the relatively greatest flood inequities occur at the 10-year event, and that inequity varies across flood magnitudes and census tracts. These findings show that using only the 100year flood zone or a single, large flood inundation scenario for a flood risk analysis can mask large inequities produced by smaller and more frequent events. Fig. 3 compares the 10-year and 100-year flood inequity scores spatially. The relative highest inequities occur at the 10-year event, implying pockets of highly vulnerable populations are concentrated close to sources of frequent flooding. For example, we found large inequities within Tract 2000 for the 10-year event, and this tract has minimal vulnerability according to the Center for Disease Control's Social Vulnerability Index (Centers for Disease Control and Prevention, 2018). In this tract, the small, non-Hispanic Black population coincided with the 10-year flooded area. We used block group data to investigate equitable exposure within the tract, and inequity was revealed that would have been missed by using data at the census tract scale. This study supports previous work that using a fine scale analysis to consider heterogeneity within a tract can reveal inequity and can supplement the CDC/ATSDR Social Vulnerability Index (Rickless et al., 2020; Rufat et al., 2019; Spielman et al., 2020; Tate et al., 2021).

We found slight differences between the 50- and 100-year events, which is similar to the findings of Liu et al. (2021) who conducted a flood risk analysis by overlaying a social vulnerability index with inundation maps from the 50-, 100-, and 200-year events separately. Their results also showed minimal differences between the events. There were slight differences between the flood depths from the First Street data for the 50- and 100-year events, shown by the same exposure values for Tracts 900, 1800, and 2100, contributing to the similar results for the

two events. We also found that the flood inequities were lower for these two events. One explanation is that as the inundation extends spread in the 50- and 100-year events, inundation reaches more of the non-socailly vulnerable population, so the overall distribution appears to be more equitable. The deterministic FEMA FIRM boundaries have led to increased development right outside of the 100-year flood zone, and the compound flood modeling from First Street captures flooding outside of this deterministic boundary (Patterson and Doyle, 2009; Wing et al., 2018). Socially vulnerable populations are more likely to reside within the FEMA FIRM 100-year flood zone than right outside of it (Chakraborty et al., 2014). As the inundation in our study expands beyond FEMA's 100-year boundary, flood exposure appears more equitable because the less vulnerable populations outside the FEMA extents are exposed for these large events.

We found that the largest and statistically significant exposure ratios occurred for the race category. These results can be explained by the legacy of systemic racism in the Southeast United States. Governments used different mechanisms such as racial zoning, road location and construction, and discriminatory housing policies to keep Black and African American populations segregated from other neighborhoods (Bayor, 1988; Linscott et al., 2021; Rothstein, 2017; Ueland and Warf, 2006). Our findings present evidence of the modern-day environmental justice implications of historical discriminatory practices.

The rankings of tracts based on damages and flood inequity were different. The tract with the greatest exposure total (Tract 2100) has FI scores close to zero, while the tracts with the greatest FI scores have lower exposure totals. We also found inequitable distribution of flooding for all but one tract, and even though less severe, the smaller inequalities reveal concerns that need remedying. Our findings emphasize the importance of prioritizing an equity analysis when assessing flood risk. If mitigation efforts are targeted based solely on flood depths, the tract with equitable flood exposure would be prioritized, leaving the tracts with large inequities unaddressed, perpetuating and potentially increasing inequity in the area.

One limitation to this study is the accuracy of the flood inundation data given the necessary simplifications employed to model floods at the scale of the conterminous United States (Wing et al., 2017). For example, the model includes levees from the National Levee Database, but not local structures such as smaller levees, culverts, or bridges (Wing et al., 2017). However, the model does accurately represent flood inundation during peak flows, and we used the largest depth which was

H. Selsor et al. Anthropocene 42 (2023) 100371

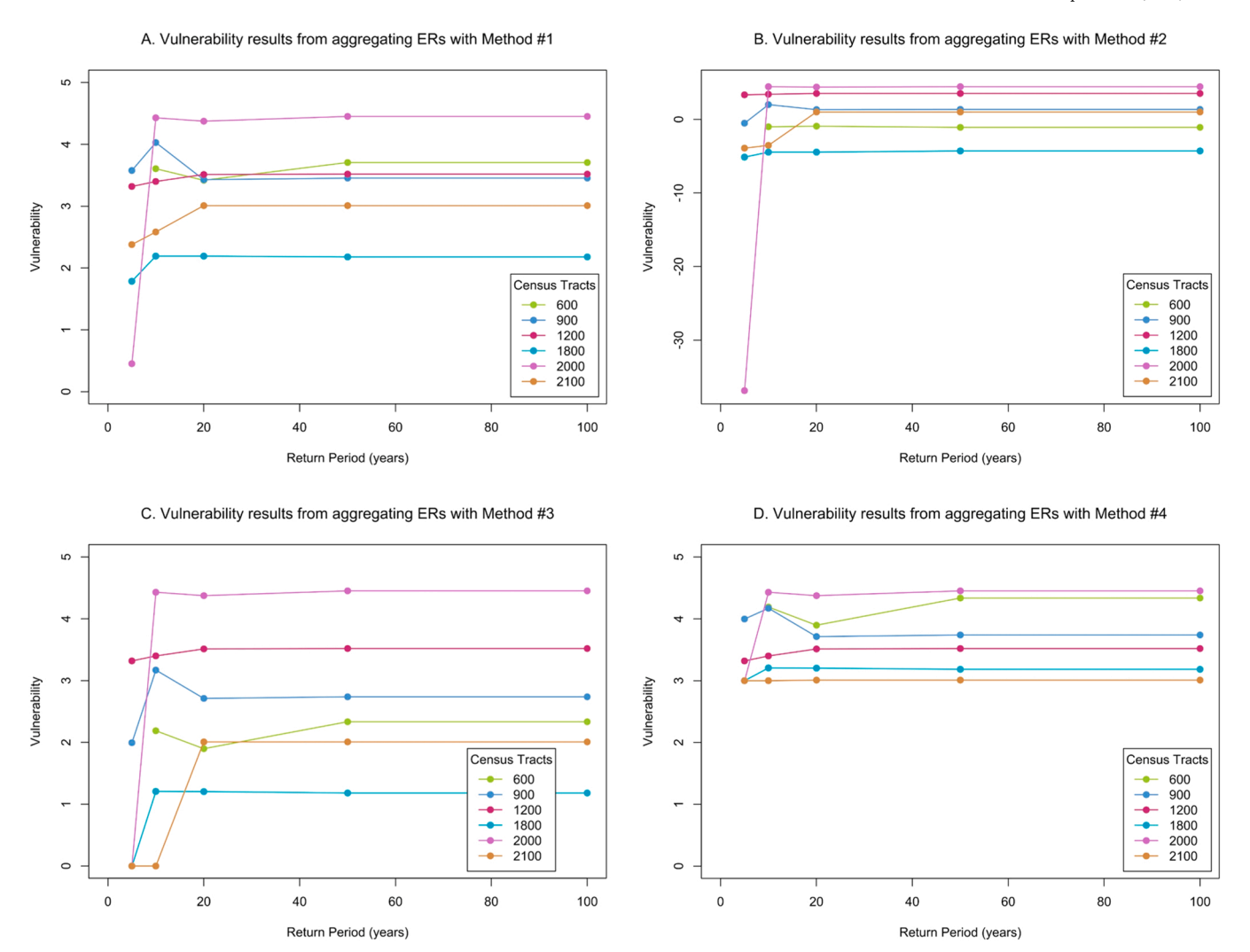


Fig. A1. The graphs of vulnerability scores from aggregating the exposure ratios with four different methods across flooding scenarios for each census tract.

likely to occur during the peak flow (Bates et al., 2021). Even though there are limitations to the modeling, the flood data we used are widely available and provide depths across multiple return periods, without which we could not have performed this analysis. Going forward, uncertainty analysis has the potential to reveal how estimated differences in exposure ratios among return periods may be affected by hydrologic and hydraulic model accuracy. The lack of uncertainty analysis, such as a Monte Carlo simulation accounting for error propagation in estimating inundation areas and depths, was not feasible within the scope of the present study and is a limitation of this research. Nevertheless, this research provides a novel framework within which uncertainty analysis could be incorporated in future studies. Even without the uncertainty analysis, there is value in demonstrating how different flood magnitudes can have unique exposure effects. Another limitation is the classification schemes employed. Exposure was classified using Jenks natural breaks and the vulnerability value was achieved through min-max normalization. While both approaches are justified, they produce FI scores that are relative to the data in the dataset, limiting the comparability of results if the same methods were applied to a different study area. To address this issue, we recommend using a human scale to categorize exposure based on where water depths hit the average human and building (e.g., knee height, chest height, first flood of a building, etc.) (Liu et al., 2021; Luke et al., 2018).

We performed a flood inequity analysis across multiple return periods using reproducible methods based on widely available data from First Street Foundation and the American Community Survey. An

advantage of the employed methods is that vulnerability calculations are specific to the exposed population at a fine scale. This differs from a social vulnerability index where vulnerability is calculated by aggregating socio-demographic characteristics, typically at a coarser scale, without differentiating the exposed area or population. The explicit inclusion of flood extents creates a social vulnerability value specific to flooding rather than general to all hazards. While a general measure of social vulnerability is useful, our approach is more fitting for a flood exposure analysis. Another advantage is that flood inequity is aggregated into a single score and not only identified spatially. This score can be used to measure the performance of mitigation efforts by quantifying resulting improvements in equity. The flood inequity score provides an additional way to evaluate flood damages besides property damage or other monetization schemes, which tend to underestimate the severity of impacts on vulnerable populations (Drakes et al., 2021; Gourevitch et al., 2020).

We recommend future work focused on developing hydrologic and hydraulic models that more accurately quantify flood inundation through greater fidelity to compound flooding mechanisms and complex flow paths. Incorporating local features will also improve accuracy as the effects of hydraulic structures have been shown to significantly affect flood depths (Stephens and Bledsoe, 2020). Another next step is to develop a method to effectively distinguish sensitivity and adaptive capacity when defining vulnerability and to incorporate a variety of socio-demographic factors such as age, health insurance, and family makeup. Additional work can identify potential solutions for reducing

Table A1Adjustment of the initial exposure ratios before their summation, shown for the four different aggregation techniques.

| Aggregation Method | s | |
|--------------------|---------------------------------------|----------------------------|
| | If exposure ratio ≤ 1 | If exposure ratio > 1 |
| Method #1 | $ER_{new} = ER_{original}$ | $ER_{new} = ER_{original}$ |
| Method #2 | $ER_{new} = \frac{-1}{ER_{original}}$ | $ER_{new} = ER_{original}$ |
| Method #3 | $ER_{new} = 0$ | $ER_{new} = ER_{original}$ |
| Method #4 | $ER_{new} = 1$ | $ER_{new} = ER_{original}$ |

inequitable flood risk. For example, green infrastructure has been shown to effectively reduce stormwater volumes and peak flow rates for smaller, more frequent events (Hoghooghi et al., 2018; Lammers et al., 2022). Green infrastructure may therefore be effective at reducing the flood inequities, which were the highest for these types of events (Hopkins et al., 2020; Woznicki et al., 2018).

5. Conclusions

Our findings show that (1) flood inequities vary according with flood magnitude and the behavior depends on the demographic distribution in the tract and (2) the 10-year event produced the greatest flood inequities. We found that the worst-case scenario of flood depths and extents does not necessarily correspond to the worst-case scenario of flood inequity, and these results have implications for flood planning and mitigation. Using flood depths alone to prioritize areas for flood mitigation can further perpetuate inequity for vulnerable populations. Vulnerable populations are facing inequitable flood exposure and possess a lower capacity to recover from floods due to a lack of resources to bear the costs of flood damages; thus, exposure to flooding can perpetuate the cycle of poverty (Coninx and Bachus, 2021; Rufat et al., 2015). Vulnerable communities are willing to move out of flood prone areas, but experience difficulties in doing so (Welch-Devine and Orland, 2020). These vulnerable communities are aware of the flood risk they are facing, but due to "chronic underprivileged circumstance" they are unable to take action to protect themselves (Harlan et al., 2019). Flood equity analyses can be used in decision-making and planning to address inequity and increase flood resiliency for all members of a community.

Declaration of Competing Interest

The authors declare that they have no known competing financial interests or personal relationships that could have appeared to influence the work reported in this paper.

Data availability

The authors do not have permission to share data.

Acknowledgments

This work was supported by the US Army Corps of Engineers Engineering With Nature $\mbox{\footnote{thmu}{B}}$ Initiative through Cooperative Ecosystem Studies Unit Agreement W912HZ-20-2-0031, the NSF Sustainability Research Network Cooperative Agreement 1444758, Urban Water Innovation Network, , and an AT&T Climate Resiliency Community Challenge grant.

Appendix

see Fig. A1. see Table A1.

Method 1 was simply summing up the three ERs. In methods 2, 3, and 4, the ratios less than one were reassigned a different value before

summing as described in Table A1. Ratios less than one indicate that there is not a vulnerable population overrepresented, and we reassigned values to prevent them from masking over-represented populations.

Method 4 is the most appropriate aggregation method based on a comparison of vulnerability scores to in statistical significance of the ERs (Fig. A1). Method 1 is straightforward, but when all three ratios for a census tract are very close to one (within 0.9–1.1), it appears to have the same vulnerability as a tract that has one, large ER with the other two ratios under one. For example, Tract 1200 has all three ERs very close to 1.0 in almost every scenario while Tract 600 has ERs greater than 2.0 that are statistically significant. With Method 1, the two appear to have similar vulnerability across the return periods, even though Tract 1200 has a proportional presence of vulnerable populations in the flood zone.

Method 2 masks large ERs, and ratios close to zero were very large when taking the inverse. For the 20-year event, Tracts 2100 and 1200 appear to have vulnerability as high as Tract 2000 even though their ERs are not much greater than one or statistically significant. Tracts 600 and 900 appear to have lower flood vulnerability than other tracts even though both have statistically significant over-representation of vulnerable populations. Method 3 also erroneously represents vulnerability because Census Tracts 600 and 900 still appear to have relatively small vulnerability. Again, Tract 2100 appears to have higher vulnerability even though all ERs are less than or equal to one so there is equitable representation of vulnerable population inf the flood zone.

A key issue with Methods 2 and 3 is that there is no clear threshold to indicate a shift from proportional representation to over-representation of vulnerable populations. Method 4 provides this threshold by reassigning the ERs less than one a value of one which represents proportional representation in the flood zone. A vulnerability score of three indicates equitable presence in the flood zone for all demographic groups. Method 4 most accurately represents the vulnerability scores we expected based on the ERs. Tracts 600, 900, and 2000 have the greatest vulnerability score across all return periods and also have the largest, statistically significant ERs. Tract 2100, which has no ERs greater than one, has a vulnerability score of three across all return periods. For these reasons, we used Method 4 to calculate the vulnerability score in the flood inequity equation.

References

Abdrabo, K.I., Kantoush, S.A., Saber, M., Sumi, T., Habiba, O.M., Elleithy, D., Elboshy, B., 2020. Integrated methodology for urban flood risk mapping at the microscale in ungauged regions: a case study of Hurghada, Egypt. Remote Sens. 12 (21), 3548. https://doi.org/10.3390/rs12213548.

Bates, P.D., De Roo, A.P.J., 2000. A simple raster-based model for flood inundation simulation. J. Hydrol. 236 (1), 54–77 https://doi.org/10.1016/S0022 1694(00) 00278-X

Bates, P.D., Quinn, N., Sampson, C., Smith, A., Wing, O., Sosa, J., Savage, J., Olcese, G., Neal, J., Schumann, G., Giustarini, L., Coxon, G., Porter, J.R., Amodeo, M.F., Chu, Z., Lewis-Gruss, S., Freeman, N.B., Houser, T., Delgado, M., Krajewski, W.F., 2021. Combined modeling of US fluvial, pluvial, and coastal flood hazard under current and future climates. Water Resour. Res. 57 (2), 1–29. https://doi.org/10.1029/

Bayor, R.H., 1988. Roads to racial segregation. J. Urban Hist. 15 (1), 3–21. https://doi. org/10.1177/009614428801500101.

Bedient, P.B., Huber, W.C., & Vieux, B.E. (2008). Hydrology and Floodplain Analysis (4. ed. ed.). Prentice Hall.

Bigi, V., Comino, E., Fontana, M., Pezzoli, A., Rosso, M., 2021. Flood vulnerability analysis in urban context: a socioeconomic sub-indicators overview (2225 1154). Climate 9 (1), 12. https://doi.org/10.3390/cli9010012.

Centers for Disease Control and Prevention /Agency for Toxic Substances and Disease Registry/ Geospatial Research, Analysis, and Services Program. CDC/ATSDR Social Vulnerability Index 2018 Database Georgia. https://www.atsdr.cdc.gov/placeandhealth/svi/data_documentation_download.html. Accessed on August 2021.

Chakraborty, J., Tobin, G.A., Montz, B.E., 2005. Population evacuation: assessing spatial variability in geophysical risk and social vulnerability to natural hazards. Nat. Hazards Rev. 6 (1), 23–33. https://doi.org/10.1061/(ASCE)1527-6988(2005)6:1

Chakraborty, J., Collins, T.W., Montgomery, M.C., Grineski, S.E., 2014. Social and spatial inequities in exposure to flood risk in Miami, Florida. Nat. Hazards Rev. 15 (3), 4014006. https://doi.org/10.1061/(ASCE)NH.1527-6996.0000140.

Chakraborty, J., Collins, T.W., Grineski, S.E., 2019. Exploring the environmental justice implications of hurricane harvey flooding in Greater Houston, Texas. Am. J. Public Health 109 (2), 244–250. https://doi.org/10.2105/AJPH.2018.304846. H. Selsor et al. Anthropocene 42 (2023) 100371

- Chang, H., Pallathadka, A., Sauer, J., Grimm, N.B., Zimmerman, R., Cheng, C., Iwaniec, D.M., Yeowon, K., Llyod, R., McPhearson, T., Rosenzweig, B., Troxler, T., Welty, C., Brenner, R., Herreros-Cantis, P., 2021. Assessment of urban flood vulnerability using the social-ecological-technological systems framework in six US cities. Sustain. Cities Soc. 68. https://doi.org/10.1016/j.scs.2021.102786.
- Collins, T.W., Grineski, S.E., Chakraborty, J., Flores, A.B., 2019. Environmental injustice and Hurricane Harvey: a household-level study of socially disparate flood exposures in Greater Houston, Texas, USA (Pt A). Environ. Res. 179, 108772. https://doi.org/ 10.1016/j.envres.2019.108772.
- Coninx, I. & Bachus, K. (2021). Integrating social vulnerability to floods in a climate change context.
- Convery, I., Bailey, C., 2008. After the flood: the health and social consequences of the 2005 Carlisle flood event. J. Flood Risk Manag. 1 (2), 100–109, 10.1111/j.1753 318X.2008.00012.x
- Cutter, S.L., Boruff, B.J., Shirley, L.W., 2003. Social vulnerability to environmental hazards. Soc. Sci. Q. 84 (2), 242–261 https://doi.org/10.1111/1540-6237.8402002.
- Debbage, N., 2019. Multiscalar spatial analysis of urban flood risk and environmental justice in the Charlanta megaregion, USA. Anthropocene 28, 100226. https://doi. org/10.1016/j.ancene.2019.100226.
- Drakes, O., Tate, E., Rainey, J., Brody, S., 2021. Social vulnerability and short-term disaster assistance in the United States. Int. J. Disaster Risk Reduct. 53, 102010 https://doi.org/10.1016/j.ijdrr.2020.102010.
- Esri Inc. (2015). ArcMap (Version 10.3.1). Esri Inc. https://www.esri.com/en-us/arcgis/products/arcgis-pro/overview.
- First Street Foundation. (2020, June 16). First Street Foundation Flood Model (FSF-FM)
 Technical Documentation. https://assets.firststreet.org/uploads/2020/06/FSF_
 Flood_Model_Technical_Documentation.pdf.
- Gourevitch, J.D., Singh, N.K., Minot, J., Raub, K.B., Rizzo, D.M., Wemple, B.C., Ricketts, T.H., 2020. Spatial targeting of floodplain restoration to equitably mitigate flood risk. Glob. Environ. Change 61. https://doi.org/10.1016/j. gloenycha 2020 102050
- Hadipour, V., Vafaie, F., Kerle, N., 2020. An indicator-based approach to assess social vulnerability of coastal areas to sea-level rise and flooding: a case study of Bandar Abbas city, Iran. Ocean Coast. Manag. 188, 105077 https://doi.org/10.1016/j. ocecoaman.2019.105077.
- Harlan, S.L., Sarango, M.J., Mack, E.A., Stephens, T.A., 2019. A survey-based assessment of perceived flood risk in urban areas of the United States. Anthropocene 28, 100217. https://doi.org/10.1016/j.ancene.2019.100217.
- Harner, J., Warner, K., Pierce, J., Huber, T., 2002. Urban environmental justice indices.
 Prof. Geogr. 54 (3), 318–331. https://doi.org/10.1111/0033-0124.00333.
 Hoghooghi, N., Golden, H.E., Bledsoe, B.P., Barnhart, B.L., Brookes, A.F., Djang, K.S.,
- Hoghooghi, N., Golden, H.E., Bledsoe, B.P., Barnhart, B.L., Brookes, A.F., Djang, K.S., Halama, J.J., McKane, R.B., Nietch, C.T., Pettus, P.P., 2018. Cumulative effects of low impact development on watershed hydrology in a mixed land-cover system. Water 10 (8), 991. https://doi.org/10.3390/w10080991.
- Hollis, G.E., 1975. The effect of urbanization on floods of different recurrence interval. Water Resour. Res. 11 (2), 431–435. https://doi.org/10.1029/WR011i003p00431.
- Homer, Collin, G., Dewitz, Jon, A., Jin, Suming, Xian, George, Costello, C., Danielson, Patrick, Gass, L., Funk, M., Wickham, J., Stehman, S., Auch, Roger, F., Ritters, K.H., 2020. Conterminous United States land cover change patterns 2001–2016 from the 2016 National Land Cover Database (at). ISPRS J. Photogramm. Remote Sens. v. 162, 184–199. https://doi.org/10.1016/j.isprsjprs.2020.02.019.
- Hopkins, K.G., Bhaskar, A.S., Woznicki, S.A., Fanelli, R.M., 2020. Changes in event based streamflow magnitude and timing after suburban development with infiltration based stormwater management. Hydrol. Process. 34 (2), 387–403. https://doi.org/ 10.1002/hyp.13593.
- Huang, H., Cheng, S., Wen, J., Lee, J., 2007. Effect of growing watershed imperviousness on hydrograph parameters and peak discharge. Hydrol. Process. 22 (13), 2075–2085. https://doi.org/10.1002/hyp.6807.
- Joyce, J., Chang, N., Harji, R., Ruppert, T., 2018. Coupling infrastructure resilience and flood risk assessment via copulas analyses for a coastal green-grey-blue drainage system under extreme weather events. Environ. Model. Softw. 100, 82–103. https:// doi.org/10.1016/j.envsoft.2017.11.008.
- Kaźmierczak, A., Cavan, G., 2011. Surface water flooding risk to urban communities: analysis of vulnerability, hazard and exposure. Landsc. Urban Plan. 103 (2), 185–197. https://doi.org/10.1016/j.landurbplan.2011.07.008.
- KC, B., Shepherd, J.M., Gaither, C.J., 2015. Climate change vulnerability assessment in Georgia. Appl. Geogr. 62, 62–74. https://doi.org/10.1016/j.apgeog.2015.04.007.
- Koks, E.E., Jongman, B., Husby, T.G., Botzen, W.J.W., 2015. Combining hazard, exposure and social vulnerability to provide lessons for flood risk management. Environ. Sci. Policy 47, 42–52. https://doi.org/10.1016/j.envsci.2014.10.013.
- Kron, W., 2005. Flood risk = hazard values vulnerability, 68 Water Int. 30 (1), 58. https://doi.org/10.1080/02508060508691837.
- Kunkel, K.E., Karl, T.R., Easterling, D.R., Redmond, K., Young, J., Yin, X., Hennon, P., 2013. Probable maximum precipitation and climate change. Geophys. Res. Lett. 40 (7), 1402–1408. https://doi.org/10.1002/grl.50334.
- Künzler, M., Huggel, C., Ramírez, J.M., 2012. A risk analysis for floods and lahars: case study in the Cordillera Central of Colombia, 796. Nat. Hazards 64 (1), 767. https:// doi.org/10.1007/s11069-012-0271-9.
- Lammers, R., Miller, L., Bledsoe, B., 2022. Effects of design and climate on bioretention effectiveness for watershed-scale hydrologic benefits. J. Sustain. Water Built Environ. 8 (4), 04022011. https://doi.org/10.1061/JSWBAY.0000993.
- Linscott, G., Rishworth, A., King, B., Hiestand, M.P., 2021. Uneven experiences of urban flooding: examining the 2010 Nashville flood. Nat. Hazards. https://doi.org/ 10.1007/s11069-021-04961-w.
- Liu, W., Hsieh, T., Liu, H., 2021. Flood risk assessment in urban areas of Southern Taiwan. Sustainability 13 (6), 3180. https://doi.org/10.3390/su13063180.

Luke, A., Sanders, B.F., Goodrich, K.A., Feldman, D.L., Boudreau, D., Eguiarte, A., Serrano, K., Reyes, A., Schubert, J.E., AghaKouchak, A., Basolo, V., Matthew, R.A., 2018. Going beyond the flood insurance rate map: insights from flood hazard map co production. Nat. Hazards Earth Syst. Sci. 18 (4), 1097–1120. https://doi.org/ 10.5194/nhess-18-1097-2018.

- Maantay, J., Maroko, A., 2009. Mapping urban risk: flood hazards, race, & environmental justice in New York. Appl. Geogr. 29 (1), 111–124. https://doi.org/ 10.1016/j.apgeog.2008.08.002.
- Mason, L.R., Ellis, K.N., Hathaway, J.M., 2017. Experiences of urban environmental conditions in socially and economically diverse neighborhoods. J. Community Pract. 25 (1), 48–67. https://doi.org/10.1080/10705422.2016.1269250.
- Moftakhari, H.R., AghaKouchak, A., Sanders, B.F., Matthew, R.A., 2017. Cumulative hazard: the case of nuisance flooding. Earth's Future 5 (2), 214–223. https://doi. org/10.1002/2016EF000494.
- Moftakhari, H.R., AghaKouchak, A., Sanders, B.F., Allaire, M., Matthew, R.A., 2018.
 What is nuisance flooding? Defining and monitoring an emerging challenge. Water Resour. Res. 54 (7), 4218–4227. https://doi.org/10.1029/2018WR022828.
- Moreira, L.L., Kobiyama, M., de Brito, M.M., 2021. Effects of different normalization, aggregation, and classification methods on the construction of flood vulnerability indexes. -98 Water 13 (98), 98. https://doi.org/10.3390/w13010098.
- Nakazawa, M. (2019). fmsb: Functions for Medical Statistics Book with some Demographic Data. R package version 0.7.0. https://CRAN.R-project.org/package=fmsb.
- Nelson, K.S., Abkowitz, M.D., Camp, J.V., 2015. A method for creating high resolution maps of social vulnerability in the context of environmental hazards. Appl. Geogr. 63, 89–100. https://doi.org/10.1016/j.apgeog.2015.06.011.
- Patterson, L.A., Doyle, M.W., 2009. Assessing effectiveness of national flood policy through spatiotemporal monitoring of socioeconomic exposure. J. Am. Water Resour. Assoc. 45 (1), 237–252, 10.1111/j.1752 1688.2008.00275.x.
- Poussard, C., Dewals, B., Archambeau, P., Teller, J., 2021. Environmental inequalities in flood exposure: a matter of scale. Front. Water 3 (633046), 1–14. https://doi.org/ 10.3389/frwa.2021.633046.
- Preisser, M., Passalacqua, P., Bixler, R.P., Hofmann, J., 2022. Intersecting fluvial and pluvial inundation estimates with sociodemographic vulnerability to quantify household risk in urban areas. Author Prepr.
- Qiang, Y., 2019. Disparities of population exposed to flood hazards in the United States.

 J. Environ. Manag. 232, 295–304. https://doi.org/10.1016/j.jenvman.2018.11.039.
- R Core Team (2022). R: a language and environment for statistical computing. R Foundation for Statistical Computing, Vienna, Austria. https://www.R-project.org/.
- Rabosky, D.L., Grundler, M.C., Anderson, C.J., Title, P.O., Shi, J.J., Brown, J.W., Huang, H., Larson, J.G., 2014. BAMMtools: an R package for the analysis of evolutionary dynamics on phylogenetic trees. Methods Ecol. Evol. 5, 701–707 https://doi.org/10.1111/2041-210X.12199.
- Rickless, D.S., Yao, X.A., Orland, B., Welch-Devine, M., 2020. Assessing social vulnerability through a local lens: an integrated geovisual approach. Ann. Am. Assoc. Geogr. 110 (1), 36–55 https://doi.org/10.1080/246944 52.2019.1625750.
- Rothstein, R. (2017). The Color of Law: A Forgotten History of How Our Government Segregated America.
- Rufat, S., Tate, E., Burton, C.G., Maroof, A.S., 2015. Social vulnerability to floods: review of case studies and implications for measurement (Part 4). Int. J. Disaster Risk Reduct. 14, 470–486. https://doi.org/10.1016/j.ijdrr.2015.09.013.
- Rufat, S., Tate, E., Emrich, C.T., Antolini, F., 2019. How valid are social vulnerability models. Ann. Am. Assoc. Geogr. 109 (4), 1131–1153. https://doi.org/10.1080/ 24694452 2018 1535887
- Schuster-Wallace, C.J., Murray, S.J., McBean, E.A., 2018. Integrating social dimensions into flood cost forecasting. Water Resour. Manag. 32 (9), 3175–3187. https://doi.org/10.1007/s11269-018-1983-8.
- Selsor, H., Lammers, R., Bledsoe, B., Jones, S., & Risse, M. (2021). Strengthening Athens-Clarke County, Georgia's Resilience to Future Flood Risks. AT&T Climate Resiliency Community Challenge Grant.
- Shepherd, M., KC, B., 2015. Climate Change and African Americans in the USA. Geogr. Compass 9 (11), 579–591. https://doi.org/10.1111/gec3.12244.
- Spielman, S.E., Folch, D., Nagle, N., 2014. Patterns and causes of uncertainty in the American Community Survey. Appl. Geogr. 46, 147–157. https://doi.org/10.1016/j. apgeog.2013.11.002.
- Spielman, S.E., Tuccillo, J., Folch, D.C., Schweikert, A., Davies, R., Wood, N., Tate, E., 2020. Evaluating social vulnerability indicators: criteria and their application to the Social Vulnerability Index. Nat. Hazards 100 (1), 417–436. https://doi.org/10.1007/s11069-019-03820-z.
- Stephens, T.A., Bledsoe, B.P., 2020. Probabilistic mapping of flood hazards: depicting uncertainty in streamflow, land use, and geomorphic adjustment. Anthropocene 29. https://doi.org/10.1016/j.ancene.2019.100231.
- Tascón-González, L., Ferrer-Julià, M., Ruiz, M., García-Meléndez, E., 2020. Social vulnerability assessment for flood risk analysis. Water 12 (2), 588. https://doi.org/ 10.3390/w12020558.
- Tate, E., 2012. Social vulnerability indices: a comparative assessment using uncertainty and sensitivity analysis. Nat. Hazards 63 (2), 325–347 https://doi.org/10.1007/s11069-012-0152-2.
- $Tate, E., 2013. \ Uncertainty \ analysis for a social vulnerability index. \ Ann. \ Assoc. \ Am. \ Geogr. \ 103 \ (3), 526-543 \ https://doi.org/10.1080/00045608.2012. \ 700616.$
- Tate, E., Rahman, M.A., Emrich, C.T., Sampson, C.C., 2021. Flood exposure and social vulnerability in the United States. Nat. Hazards 106 (1), 435–457. https://doi.org/ 10.1007/s11069-020-04470-2.
- Trenberth, K.E., 2011. Changes in precipitation with climate change. Clim. Res. 47 (1/2), 123–138. https://doi.org/10.3354/cr00953.

- Tyagi, P., 2020. Flood risk, coastal megacities, and urban poor: assessing the future urban flood risk in the h/e ward of Mumbai. J. Urban Environ. Eng. 14 (2), 192–203. https://doi.org/10.4090/juee.2020.v14n2.192203.
- U.S. Census Bureau (2019c). B17017: poverty status in the past 12 months by household type by age of householders. https://data.census.gov/cedsci/ table? q=b17017&g=0500000US13059%241500000&tid=ACSDT5Y2018.B17017.
- U.S. Census Bureau (2019a). B02001:RACE. https://data.census.gov/cedsci/table? q=b0200 1&g=0500000US13059%241500000&tid=ACSDT5Y2018.B02001.
- U.S. Census Bureau (2019b). B03003: hispanic or latino origin. https://data.census.gov/cedsci/table?q=b03003&g=0500000US13059%241500000&tid=ACSDT5Y20. B03003.
- Ueland, J., Warf, B., 2006. Racialized topographies: altitude and race in southern cities. Geogr. Rev. 96 (1), 50–78 https://doi.org/10.1111/j.1931- 0846.2006.tb00387.x.
- United Nations Population Division. (2008). United Nations expert group meeting on Population Distribution, Urbanization, Internal Migration and Development. United Nations Secretariat, p. 7.
- Vicente, B., Menéndez, A., Natenzon, C., Kokot, R., Codignotto, J., Re, M., Bronstein, P., Camilloni, I., Ludueña, S., González, S.G., Ríos, D.M., 2006. Vulnerability to floods in the metropolitan region of Buenos Aires under future climate change. Assessments of Impacts and Adaptations to Climate Change (AIACC), Working Paper (26).
- Welch-Devine, M., Orland, B., 2020. Is it itime to move away? How hurricanes affect future plans. Int. J. Mass Emergencies Disasters 38 (1), 54–76.
- Wilson, B., Tate, E., Emrich, C.T., 2021. Flood recovery outcomes and disaster assistance barriers for vulnerable populations. Front. Water. 310.3389/frwa.2021.752307.

Wing, O.E.J., Bates, P.D., Sampson, C.C., Smith, A.M., Johnson, K.A., Erickson, T.A., 2017. Validation of a 30 m resolution flood hazard model of the conterminous United States. Water Resour. Res. 53, 7968–7986 https://doi.org/10.1002/2017WR 020017

Anthropocene 42 (2023) 100371

- Wing, O.E.J., Bates, P.D., Smith, A.M., Sampson, C.C., Johnson, K.A., Fargione, J., Morefield, P., 2018. Estimates of present and future flood risk in the conterminous United States. Environ. Res. Lett. 13 https://doi.org/10.1088/1748-9326/aaac65.
- Wing, O.E.J., Lehman, W., Bates, P.D., Sampson, C.C., Quinn, N., Smith, A.M., Neal, J.C., Porter, J.R., Kousky, C., 2022. Inequitable patterns of US flood risk in the Anthropocene. Nat. Clim. Change 12, 156–162 https://doi.org/10.1038/s41558 -021-01265-6.
- Woznicki, S.A., Hondula, K.L., Jarnagin, S.T., 2018. Effectiveness of landscape-based green infrastructure for stormwater management in suburban catchments. Hydrol. Process. 32 (15), 2346–2361. https://doi.org/10.1002/hyp.13144.
- Yang, Q., Zhang, S., Dai, Q., Yao, R., 2020. Improved framework for assessing vulnerability to different types of urban floods. Sustainability 12 (18), 7668. https://doi.org/10.3390/su12187668.
- Ye, C., Xu, Z., Lei, X., Liao, W., Ding, X., Liang, Y., 2022. Assessment of urban flood risk based on data-driven models: a case study in Fuzhou City, China. Int. J. Disaster Risk Reduct. 82, 103318 https://doi.org/10.1016/j.ijdrr.2022.103318.
- Zhou, Q., Leng, G., Su, J., Ren, Y., 2019. Comparison of urbanization and climate change impacts on urban flood volumes: importance of urban planning and drainage adaptation. Sci. Total Environ. 658, 24–33 https://doi.org/10.1016/j. scitotenv.2018.12. 184.